

N 64 10 3 38

CODE-1

NASA CR-52463

Technical Memorandum No. 33-140

*Final Report on Mariner 2
Temperature Control*

D. W. Lewis

M. B. Gram

R. J. Spehalski

L. N. Dumas



JET PROPULSION LABORATORY
CALIFORNIA INSTITUTE OF TECHNOLOGY
PASADENA, CALIFORNIA

July 1, 1963

REPRODUCED BY
NATIONAL TECHNICAL
INFORMATION SERVICE
U.S. DEPARTMENT OF COMMERCE
SPRINGFIELD, VA. 22161

Technical Memorandum No. 33-140


*1. Final Report on Mariner 2
Temperature Control*

D. W. Lewis ,

M. B. Gram ,

R. J. Spehalski,

L. N. Dumas


W. J. Schimandle, Chief
Spacecraft Development Section

474 2003

JET PROPULSION LABORATORY
CALIFORNIA INSTITUTE OF TECHNOLOGY
PASADENA, CALIFORNIA)

July 1, 1963

Copyright © 1963
Jet Propulsion Laboratory
California Institute of Technology

Prepared Under Contract No. NAS 7-100
National Aeronautics & Space Administration

CONTENTS

| | |
|--|----|
| I. Introduction | 1 |
| II. Design Philosophy | 2 |
| III. Design Details | 6 |
| IV. Predicted Flight Performance | 8 |
| V. Flight Performance | 9 |
| VI. Analysis of Flight Performance | 11 |
| VII. Conclusion | 14 |
| Appendix | 15 |

TABLES

| | |
|--|----|
| 1. Predicted and flight temperatures | 12 |
| A-1. Sequence of significant flight events | 15 |

FIGURES

| | |
|---|----|
| 1. <i>Mariner R</i> configuration showing temperature-control components: | |
| (a) Radiometer side | 3 |
| (b) Long-range Earth-sensor side | 4 |
| A-1. Solar intensity at <i>Mariner 2</i> spacecraft | 16 |
| A-2. <i>Mariner 2</i> louver position | 16 |
| A-3. <i>Mariner 2</i> power boost-regulator temperature | 17 |

FIGURES (Cont'd)

| | |
|---|----|
| A-4. <i>Mariner 2</i> propulsion-system nitrogen-tank temperature | 17 |
| A-5. <i>Mariner 2</i> propellant-tank temperature | 18 |
| A-6. <i>Mariner 2</i> Earth-sensor temperature | 18 |
| A-7. <i>Mariner 2</i> battery temperature | 19 |
| A-8. <i>Mariner 2</i> attitude-control system nitrogen-tank temperature | 19 |
| A-9. <i>Mariner 2</i> 4A11 and 4A12 solar-panel front temperatures | 20 |
| A-10. <i>Mariner 2</i> 4A11 solar-panel back temperature | 20 |
| A-11. <i>Mariner 2</i> electronic assembly I temperature (power boost-regulator and science assemblies) | 21 |
| A-12. <i>Mariner 2</i> electronic assembly II temperature (transponder) | 21 |
| A-13. <i>Mariner 2</i> electronic assembly III temperature (data encoder and command) | 22 |
| A-14. <i>Mariner 2</i> electronic assembly IV temperature (CC&S and attitude control) | 22 |
| A-15. <i>Mariner 2</i> electronic assembly V temperature (power and pyrotechnics assemblies) | 23 |
| A-16. <i>Mariner 2</i> lower thermal shield temperature | 23 |
| A-17. <i>Mariner 2</i> upper thermal shield temperature | 24 |
| A-18. <i>Mariner 2</i> plasma experiment temperature | 24 |
| A-19. <i>Mariner 2</i> antenna yoke temperature | 25 |
| A-20. <i>Mariner 2</i> infrared radiometer housing | 25 |

ABSTRACT

10338

The basic principles and specific techniques of temperature control employed on the *Mariner R* spacecraft are presented. A chronological history of the thermal aspects of the *Mariner 2* flight is given, including telemetry data for monitored components. The significance of the data in terms of improving temperature-control techniques is discussed.

AUTHOR

I. INTRODUCTION

Ultimately, the temperature control of a spacecraft involves a thermal radiation balance of absorbed solar energy and radiant energy lost to the heat sink of space. Solar input and radiated energy will vary from surface to surface because of differences in shape and in optical properties. Moreover, a portion of the incident solar energy will be converted to electrical energy and dissipated in various spacecraft assemblies as a function of the operating mode. These factors, along with rather complex internal heat-transfer parameters, determine the spacecraft temperature distribution.

To achieve temperature control of the *Mariner R*, an effort was made to influence the design of the spacecraft in such a manner that each component would remain at an acceptable temperature throughout the mission. This function was so intimately associated with the details of internal and external spacecraft design that a list of the components of the temperature-control "system" must implicitly include a consideration of temperature effects on spacecraft structure, materials, and assembly. Salient features of the *Mariner R* temperature-control system include louvers, radiation shields, paint patterns and surface finishes, and thermal conduction insulators.

II. DESIGN PHILOSOPHY

The extreme difference in solar intensity at Earth and Venus — about 130 to 250 w/ft² — required that temperature-sensitive components be isolated from solar inputs as far as possible (see Fig. 1). Large variations in temperature (approximately 90°F) would have been experienced by a totally Sun-dependent object.

Solar inputs to the basic hexagonal enclosure (hex) were minimized by shielding normally sunlit surfaces, and the heat necessary for maintaining internal temperatures was supplied by the relatively constant internal power dissipation. Since the potential heat loss from external radiating surfaces was much larger than the internal electrical losses, exterior surfaces of poor radiating qualities (low emissivity) were generally used. Paint patterns were applied as necessary to increase emissivity near regions of high power dissipation. Internal surfaces were blackened to maximize internal transfer and to minimize assembly temperature differences. An active device (louvers) was included to vary the effective emissivity of one box face, thus further suppressing the temperature rise within the hex.

Temperature-sensitive components not enclosed within the basic hex were considered individually. For the scientific instruments, solar energy inputs were necessary to maintain reasonably warm temperatures near Earth, which resulted in large Earth-to-Venus temperature rises. The design intent was to start near the lower temperature limit at Earth to avoid excessively high encounter temperatures. The solar panels were designed to operate at the lowest possible temperature by maximizing the emissivity of the front and back surfaces and by minimizing the temperature drop across the panel. Prior to Earth acquisition, the Earth sensor was maintained at a safe temperature by an internal heater. The changing antenna hinge angle during flight had the undesirable effect of changing the solar input to the Earth sensor, but it was felt that by starting cold near Earth a fairly large temperature rise could be tolerated by this instrument.

All external cabling and structure were treated to produce both a low solar absorptivity and a low infrared emissivity. The low emissivity provided for the distribution of heat along the structure by conduction, thus leading to a more nearly isothermal condition. The low absorptivity prevented an excessive spacecraft solar dependency by means of absorbing solar energy that could have been conducted into the generally cooler hex.

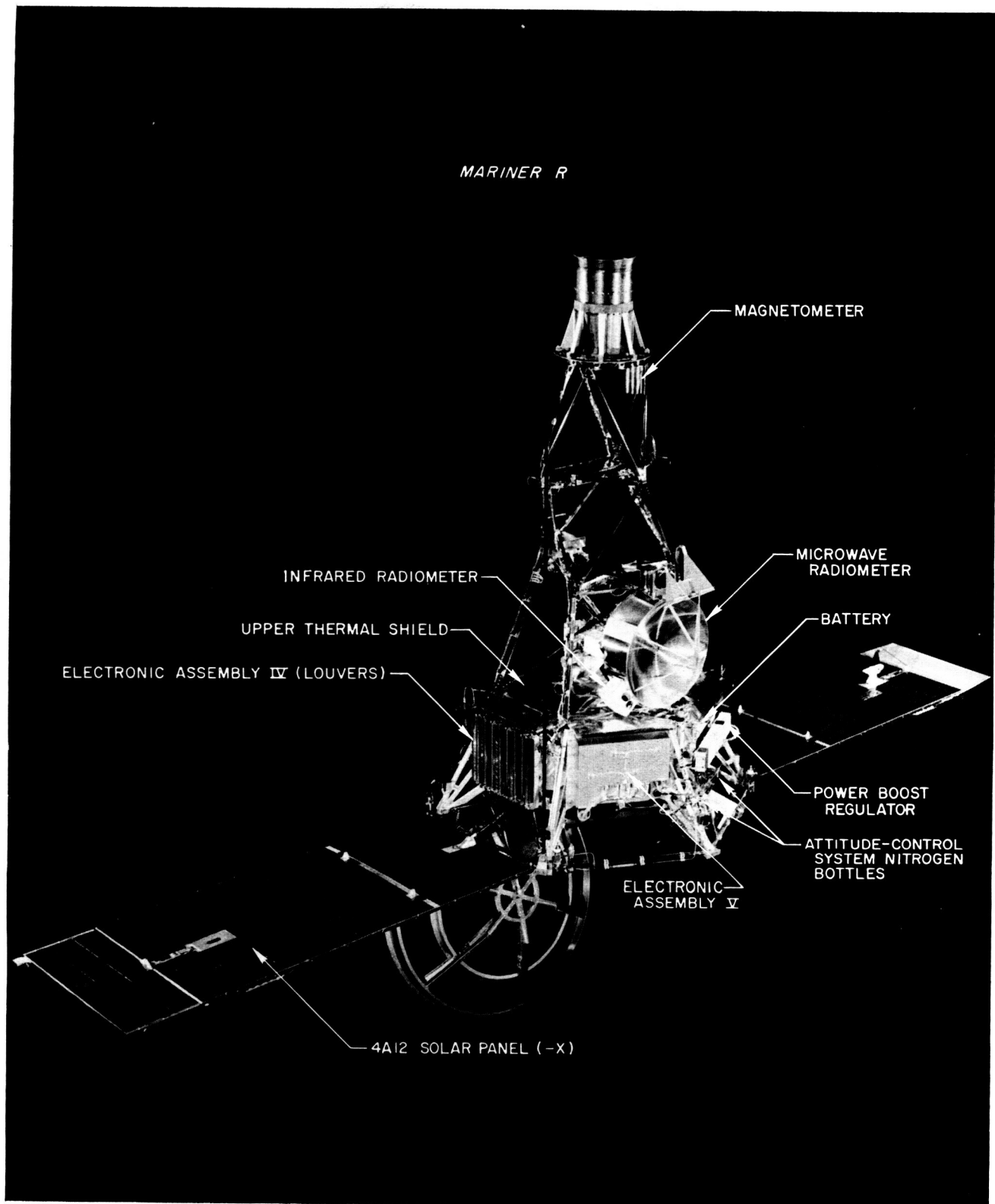


Fig. 1. *Mariner R* configuration showing temperature-control components:
(a) Radiometer side

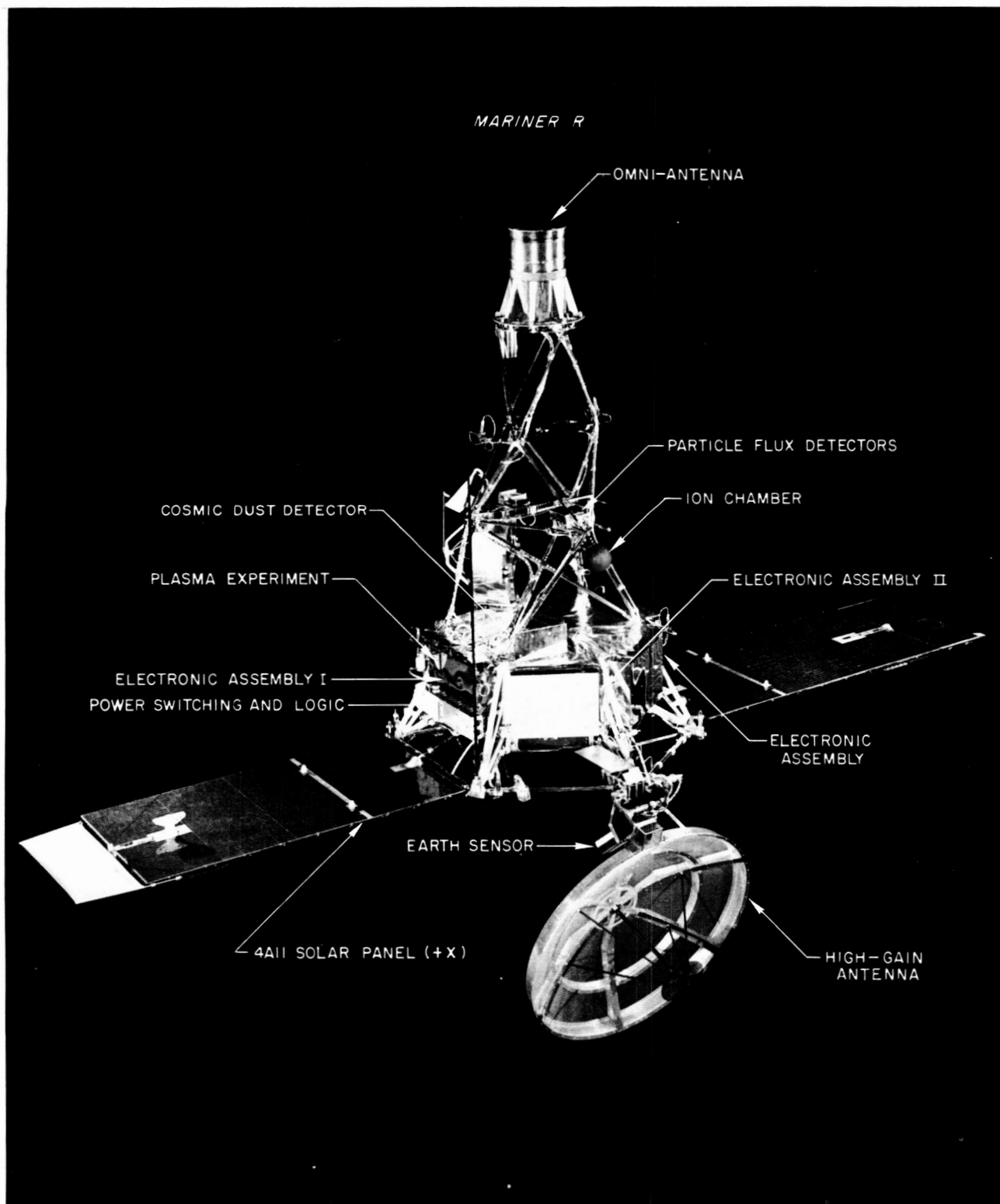


Fig. 1. *Mariner R* configuration showing temperature-control components:
(b) Long-range Earth-sensor side

The spacecraft was designed to present a highly reflective surface to the Sun during the normally Sun-oriented portions of the flight. This design required that the sides of the spacecraft be of fairly high solar absorptivity. During midcourse maneuver the solar input on the sunlit side of the spacecraft, combined with the heat from the midcourse motor, could be expected to cause a substantial increase in spacecraft temperatures, but the thermal capacity of the craft was large enough to limit the temperature rise during the relatively short period of time involved.

III. DESIGN DETAILS

The most important barrier to excessive solar inputs was the upper thermal shield, which consisted of multiple layers of aluminized Mylar supported on a Fiberglas honeycomb panel. An aluminized Teflon sheet, selected for its optical properties and its resistance to degradation by ultraviolet radiation, covered the upper surface of the shield. The result was a rigid, lightweight, and highly effective radiation shield. It was anticipated that less than 2% of the solar irradiation would be transmitted through the shield to the hex interior.

A lower thermal shield was used to minimize heat losses from the bottom of the hex enclosure. The multiple layers of aluminized Mylar were supported on a thin aluminum panel. High-temperature damage to the Mylar resulting from the firing of the midcourse motor was prevented by facing the inner side with aluminum foil. The heat loss through this shield was estimated to be about five watts.

The louvers on electronic assembly IV [Attitude Control and Central Computer and Sequencer (CC&S)] fulfilled two design requirements. First, they maintained temperature-critical guidance electronic equipment within much closer limits than would otherwise have been possible with the widely varying internal power dissipation of the electronic assembly. Second, the louvers provided a variable heat valve, which compensated for out-of-tolerance temperature conditions caused by unavoidable or unforeseen factors. The louver assembly consisted of eight movable polished aluminum louvers, each individually actuated by a bimetallic element. The louvers and actuators were mounted to the electronic assembly with a support frame. With a rise in electronic assembly temperature, the bimetal elements rotated the louvers to a more open position, increasing the effective emittance of the box face and increasing the radiant flux to space. The louvers were designed to be completely closed at 60°F and fully open at 90°F, with a heat loss in these positions of 3 and 38 w, respectively. The entire louver assembly weight was less than 2 lb.

In addition to the above hardware, the temperature-control design included the specification of finishes for internal and external surfaces. Four general categories of treatment are given below:

1. *Structure and bracketry external to the basic hex.* Superstructure, hex support legs, and intercostals were gold-plated if magnesium or polished if aluminum. These finishes are poor emitters and poor absorbers of thermal radiation, and as such they contributed little to the heat balance of the structure to which they were conductively coupled. This treatment also caused the temperature of these members to respond more slowly

(longer time constant) to the thermal perturbations that occurred during the Sun acquisition and midcourse maneuver, when Sun attitude was not maintained. External cabling was included in the category. All such cabling was wrapped in aluminized Mylar, which made its thermal behavior similar to that described above.

2. *Components entirely internal to the basic hex.* Included in this group were the midcourse propulsion system, the electronic subassemblies, the internal surfaces of the electronic assembly, and interconnecting cables and connectors. These parts were all surfaced with paints or conversion coatings that made them good thermal radiators. The resultant high internal heat fluxes reduced temperature differences within the hex.
3. *The six electronic assemblies.* The electronic assemblies were treated in accordance with the internal power dissipation of each. Assemblies with high internal power were provided with a good radiating surface (ZW-60 white paint), whereas low internal power assemblies were provided with polished aluminum shields to minimize the heat loss. The effect of this treatment was to further reduce temperature differences within the hex.
4. *Nonstructural components external to the basic hex.* Science experiments, Sun sensors, and the attitude-control nitrogen system are examples. For these items passive thermal-control techniques were used, in that surface finishes were specified which balanced internal power plus absorbed solar energy with thermal radiation and conduction losses to achieve desired temperatures.

IV. PREDICTED FLIGHT PERFORMANCE

The design of the *Mariner R* did not lend itself to comprehensive analytical temperature predictions. The difficulties in generating a realistic mathematical model, coupled with uncertainties in surface properties and electrical power distribution, would have resulted in unacceptably large temperature uncertainties. In view of this lack of analytical confidence, a number of thermal tests were performed using a full-sized spacecraft in the most realistic simulation of the space environment available. This spacecraft, the Temperature Control Model (TCM), was structurally identical to the flight model, but resistors were substituted for flight electronics to simulate internal power dissipation. Tests were carried out in both the 6 by 7 ft vacuum chamber and the 25-ft space simulator, but in neither of these chambers was adequate solar simulation available. Accordingly, resistance heaters encased in thin rubber sheets were applied to sunlit surfaces to simulate solar heating. The final thermal design was based on the results of these tests.

V. FLIGHT PERFORMANCE

The prelaunch Atlantic Missile Range activity pertinent to temperature control of the *Mariner R* involved final thermal preparation and the monitoring of spacecraft temperatures during the various electrical tests and checks. Final thermal preparation consisted of insuring that all spacecraft surfaces conformed to the temperature-control design. All surfaces were meticulously cleaned where possible, but repainting of some assemblies was required. Spacecraft temperatures were monitored during the various electrical tests, and checks were made to insure that no out-of-tolerance temperature conditions were experienced. A continuous log of spacecraft and environmental temperatures was maintained. In this way, a "normal thermal condition" was established against which spacecraft temperatures were checked during countdown as an aid in detecting any abnormal condition.

Prior to launch, *Mariner 2* temperatures had stabilized at predicted levels, consistent with previous countdowns and tests. The environment within the shroud was maintained at 70°F by means of the air-conditioned shroud cooling blanket. Spacecraft temperatures at launch ranged from 70 to 109°F.

The immediate postlaunch environment of increased internal power, lack of Sun attitude, and aerodynamic heating forced spacecraft temperatures upward. Two hours after launch, temperatures were slowly decreasing. By 8 hr after launch, temperatures had essentially stabilized with an average hex temperature of 84°F.

Temperatures remained essentially constant from this time until midcourse maneuver. At that time, because of increased internal power, a significant heat input from the propulsion system, and a lack of Sun orientation, the spacecraft hex experienced an average rise in temperature of 20°F. Within 10 hr after midcourse, temperatures had decayed to pre-midcourse maneuver values. The maximum and minimum temperatures measured during the midcourse maneuver were 130 and 72°F as experienced by the midcourse nitrogen tank and upper thermal shield, respectively.

After midcourse maneuver, *Mariner 2* temperatures increased through encounter with exceptions as given below. Two exceptions were the Earth sensor and the antenna yoke, which cooled to 85°F on October 27, 1962,¹ then increased steadily in temperature. This behavior was a consequence of variable shading of these parts as the antenna hinge angle changed.

¹Day 300.

On October 31, 1962,² a solar-panel malfunction followed by an "off-science" condition resulted in a temperature decrease of the entire hex of about 5°F. Particularly affected were the booster regulator, battery, and science electronic assembly, which dropped 9, 5, and 8°F, respectively. The temperature drops were a direct result of a decrease in power dissipation within the hex. Eight days later, the solar panel returned to normal operation, and cruise science was reactivated. Within 8 hr, temperatures had regained the decrement dropped after the malfunction. On November 15, 1962,³ another solar-panel malfunction occurred. However, cruise science was not commanded off, and temperatures were only slightly affected. Solar-panel front temperatures dropped 2°F; booster regulator temperature dropped 3°F.

Temperature measurements were not telemetered during the encounter mode, but temperatures measured before and after encounter were compared to determine the thermal influence of Venus on the spacecraft. Both the battery and the power assembly indicated a 2°F temperature rise when the cruise mode was resumed. Both of these assemblies faced Venus during encounter, but part of the temperature rise resulted from increased internal power.

After encounter, spacecraft temperatures continued to rise slowly until December 28, 1962,⁴ at which time the spacecraft had reached its closest point of approach to the Sun. Before the slowly decreasing solar intensity could result in lower temperatures, however, a CC&S casualty on December 30⁵ caused a lowering of electrical efficiency within the spacecraft. The result was a sharp rise in internal power dissipation, which caused hex temperatures to rise gradually over the following 3 days. By January 2, 1963,⁶ the following temperature rises had occurred: booster regulator, 9°F; propulsion system nitrogen tank, 8°F; propellant tank, 5°F; battery, 7°F; electronic assembly I, 3°F; electronic assembly II, 3°F; electronic assembly III, 3°F; electronic assembly IV, 5°F; electronic assembly V, 17°F; upper thermal shield, 2°F. The last data received before spacecraft failure on January 3⁷ indicated no change in temperatures during the previous 17 hr.

²Day 304.

³Day 319.

⁴Day 362.

⁵Day 364.

⁶Day 002.

⁷Day 003.

VI. ANALYSIS OF FLIGHT PERFORMANCE

The *Mariner 2* flight was notable for the virtually universal high temperature condition of the spacecraft. Temperatures near Earth exceeded expectations by as much as 40°F; those near encounter were as much as 75°F high. Indeed, the only monitored temperatures that behaved as expected were those of the solar panels. Predicted and actual temperatures are given in Table I. The sequence of significant flight events and plots of temperature and data number as a function of time are included in Appendix A.

There are four general categories into which possible causes for the high temperature condition can be grouped:

1. *High internal power dissipation.* Although erroneous predictions for individual components may have been made, it is felt that no great over-all disparity between expected and actual power dissipation existed.
2. *High solar heat input.* The fact that the temperature rise between Earth and Venus was substantially higher than expected suggests that this effect was at least partially to blame for the warm condition. Two known contributions of solar input to the spacecraft were neglected in preflight testing because of the nature of the tests. One effect was that of reflected solar irradiation. For example, the energy incident on hex faces that was reflected from intercostals and legs was not provided for by the heater pad approach. Direct solar inputs were easily simulated by simply applying the appropriate heat to sunlit areas, but any similar treatment of reflected sunlight was so difficult as to be prohibitive. Another such effect was the conduction of heat into the hex from sunlit structural members. This effect, not simulated because of the small energies involved and the difficulty in implementation, was again "in the wrong direction". Also, the degradation of white paints and the upper thermal shield because of ultraviolet irradiation over the course of the flight caused an increase in total spacecraft solar absorptivity.
3. *Lowered emissivities.* Any contamination of polished surfaces by oil, dirt, etc., causes an increase in emissivity and hence in heat radiating capability. The exact nature and degree of contamination of spacecraft surfaces in vacuum chambers has proved difficult

Table 1. Predicted and flight temperatures

| Component | Temperature, °F | | | | | |
|--|--------------------|-----------|----------------------|-----------|---------------------------|-----------------------------|
| | Earth (stabilized) | | Venus | | Maximum (Jan. 2, 1963) | Desired operating limits |
| | Actual | Predicted | Actual | Predicted | | |
| Power boost regulator | 80 | 78 | 129 | 114 | 143 | 32-140 |
| Propulsion system nitrogen tank | 78 | 55 | 139 | 84 | 151 | 35-165 |
| Propellant tank | 76 | 55 | 138 | 84 | 148 | 35-165 |
| Earth sensor | 78 | 40 | 165 ^a | 90 | 171 ^a | 0-95 |
| Battery | 70 | 55 | 130 ^a | 91 | 141 | 50-120 |
| Attitude-control system nitrogen tank | 68 | 59 | 160 ^a | 115 | - | 32-140 |
| Solar panel front | 126 | 132 | 250-254 ^a | 262 | - | As cold as possible |
| Electronic assembly I | 73 | 50 | 152 | 92 | 160 | 14-149 |
| Electronic assembly II | 85 | 60 | 152 | 90 | 159 | 0-140 |
| Electronic assembly III | 86 | 62 | 149 | 89 | 157 | 0-149 |
| Electronic assembly IV | 74 | 60 | 124 | 80 | 134 | 50-130 |
| Electronic assembly V | 86 | 52 | 135 | 84 | 158 | 32-140 |
| Lower thermal shield | 58 | 32 | 122 ^a | 58 | - | - |
| Upper thermal shield | 59 | 80 | 153 | 215 | 162 | - |
| Plasma experiment (electronic assembly I) | 78 | 50 | 155 | 92 | - | 14-158 |
| ^a Extrapolated values. | | | | | | |

to assess, although certainly oil contamination is known to occur from time to time. In any case, it is possible that the "cleaning" action of the hard vacuum of space lowers emissivities to such a degree that higher temperatures result.

4. *Inadequate thermal test mockup.* Some of the difficulties encountered in preflight thermal tests have already been mentioned. An additional source of error was the localizing (in heater pads) of distributed solar inputs and the possible unbonding of the heaters from the spacecraft surface. Both of these factors could have caused local "hot-spots" that radiated heat away at high temperatures, thereby creating artificially low temperatures within the spacecraft.

VII. CONCLUSION

Despite the warmth with which *Mariner 2* greeted outer space, the thermal design proved to be fundamentally sound. The louvers performed well, decreasing the average hex temperature excursion by 12 to 15°F. All temperatures stayed within limits during the critical midcourse maneuver.

Present test techniques, however, have been shown to be inadequate for the requirements of planetary missions. A large store of flight data, which should prove invaluable in the temperature control of future generations of spacecraft, has been collected.

APPENDIX
Mariner 2 Flight Data

Table A-1. Sequence of significant flight events

| Day | Estimated time (GMT) | Event | Day | Estimated time (GMT) | Event |
|-----|----------------------|--|-----|----------------------|--|
| 239 | 06:53:14 | Liftoff | 248 | 00:01:00 | Pitch turn sequence begins |
| | 06:58:14 | Atlas-Agena separation | | 00:23:00 | Motor burn sequence begins |
| | --- | First Agena ignition | | 00:23:00 | Command motor ignition |
| | --- | First Agena burnout | | 00:23:31 | Command motor shutoff |
| | --- | Second Agena ignition | | 00:27:00 | Sun reacquisition |
| | --- | Second Agena burnout | | 00:34 | Sun reacquired |
| | 07:21:53 | Spacecraft-Agena separation | | 00:34 | Gyros turned off |
| | 07:37:04 | Unfold solar panels and unlatch radiometer | | 00:34 | Cruise science turned on |
| | 07:38:07 | Solar panels unfolded | | 02:07:53 | Earth reacquisition |
| | 07:53:07 | Initial Sun acquisition | | 02:34 | Earth reacquired |
| | 07:55:35 | Sun acquired | 304 | 05:30 | Power failure |
| | 07:58:35 | Gyros turned off | | 20:28 | Transmitted RTC-10 (cruise science off) |
| 241 | 16:13:00 | Transmitted RTC-8 (cruise science on) | 312 | 01:00 | Power system operating normally |
| 246 | 05:29:14 | Initial Earth acquisition | | 21:26 | Transmitted RTC-8 (cruise science on) |
| | 05:29:14 | Earth sensor power turned on | | | |
| | 05:29:14 | Gyros turned on | 313 | 12:22 | Power failure |
| | 05:29:14 | Cruise science turned off | | | |
| | 05:29:14 | Initiate roll search | 343 | 23:20 | Data encoder malfunction |
| | 05:58:58 | Earth acquired | 346 | 20:01 | CC&S failure |
| | 05:58:58 | Roll search stops | | | |
| | 05:58:58 | Gyros turned off | 348 | --- | Encounter phase sequence |
| | 05:58:58 | Cruise science turned on | | 13:35 | Transmitted RTC-7 (encounter telemetry mode) |
| 247 | 22:49:42 | Transmitted RTC-6 (initiate midcourse maneuver sequence) | | 20:39 | Transmitted RTC-8 (cruise science on) |
| | 22:49:42 | Accelerometer turned on | | | |
| | 22:49:42 | Gyros turned on | 364 | 17:28 | CC&S or power system failure frequency shift |
| | 22:49:42 | Cruise science turned off | 003 | 07:00 | Spacecraft's last received signal |
| | 23:49:00 | Roll turn sequence begins | | | |

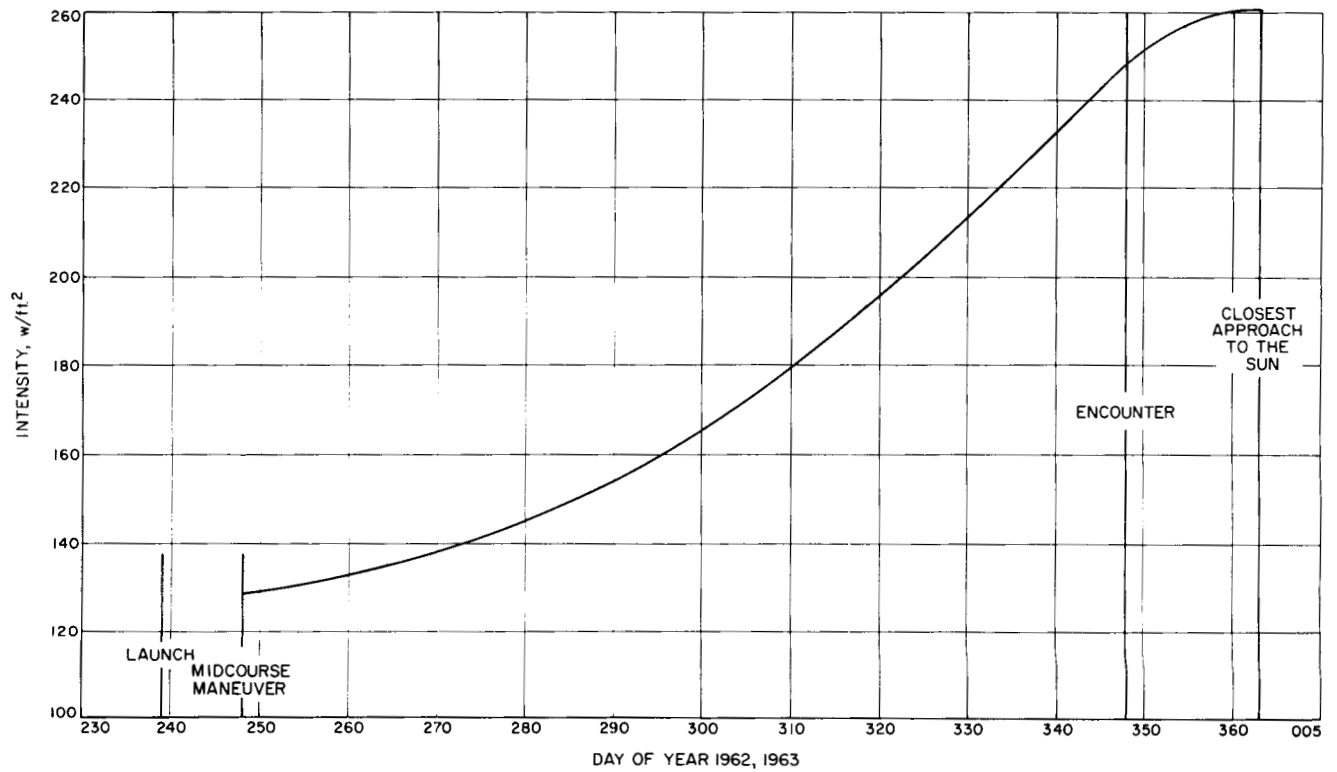


Fig. A-1. Solar intensity at *Mariner 2* spacecraft

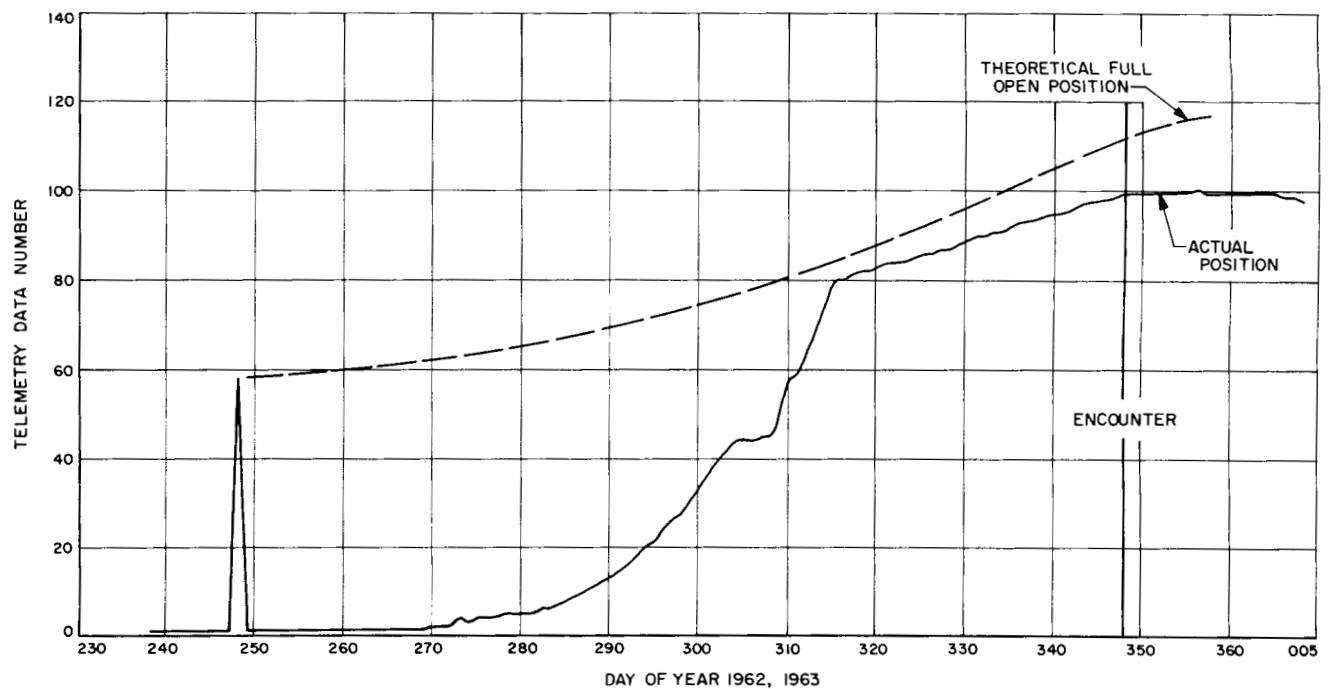


Fig. A-2. *Mariner 2* louver position

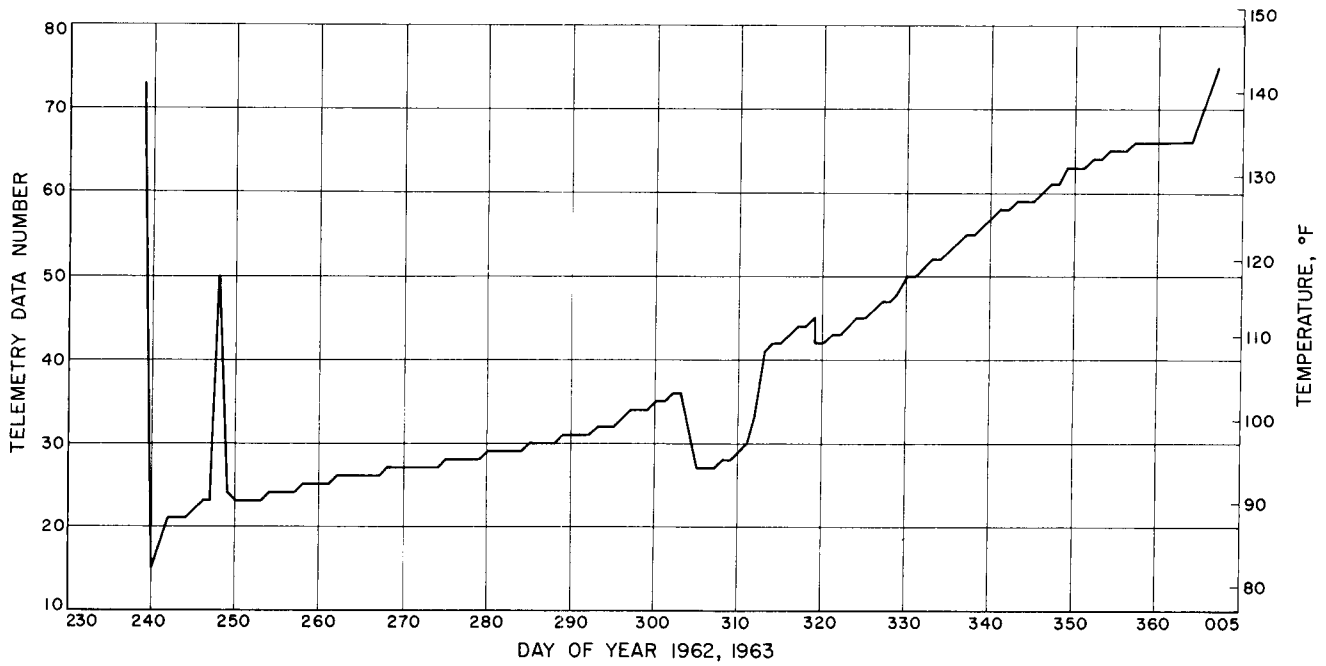


Fig. A-3. *Mariner 2* power boost-regulator temperature

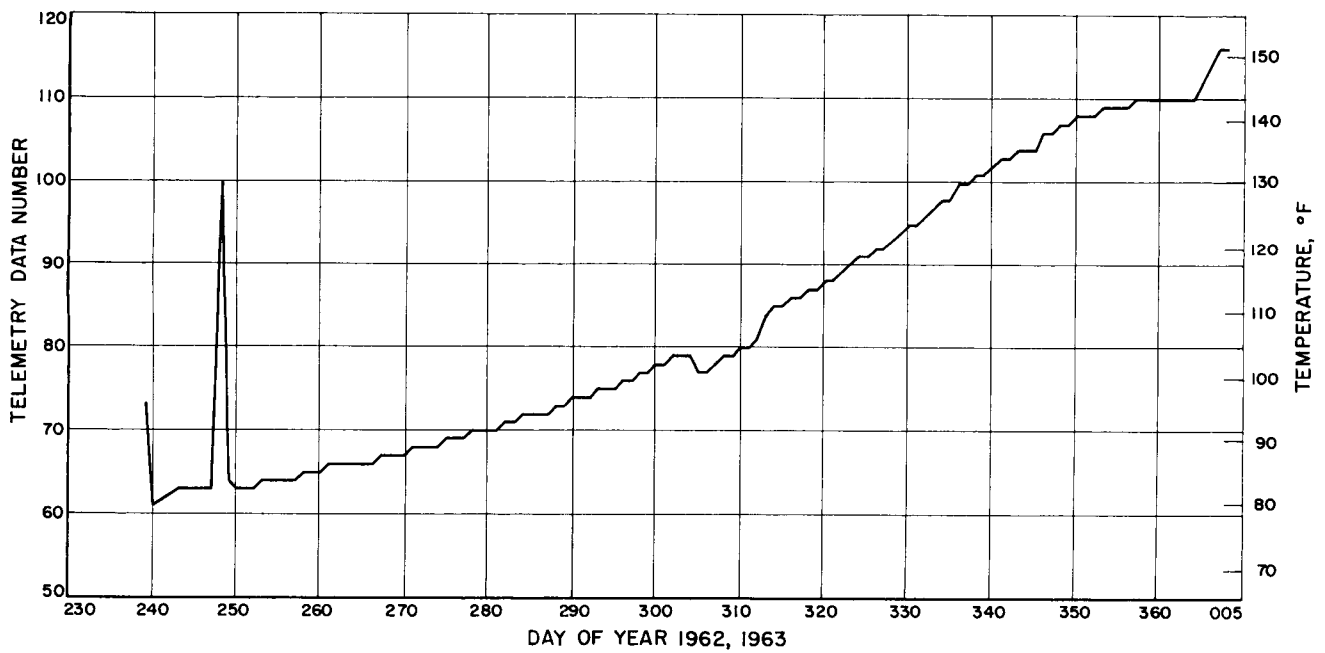


Fig. A-4. *Mariner 2* propulsion-system nitrogen-tank temperature

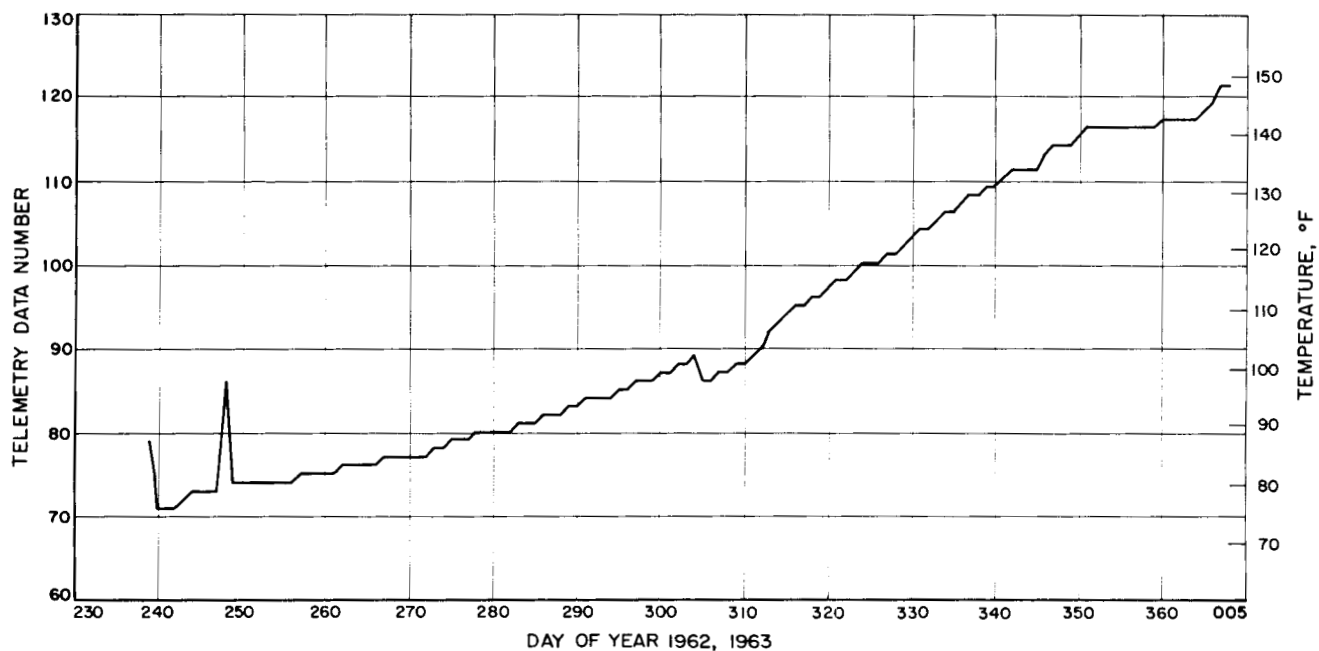


Fig. A-5. *Mariner 2* propellant-tank temperature

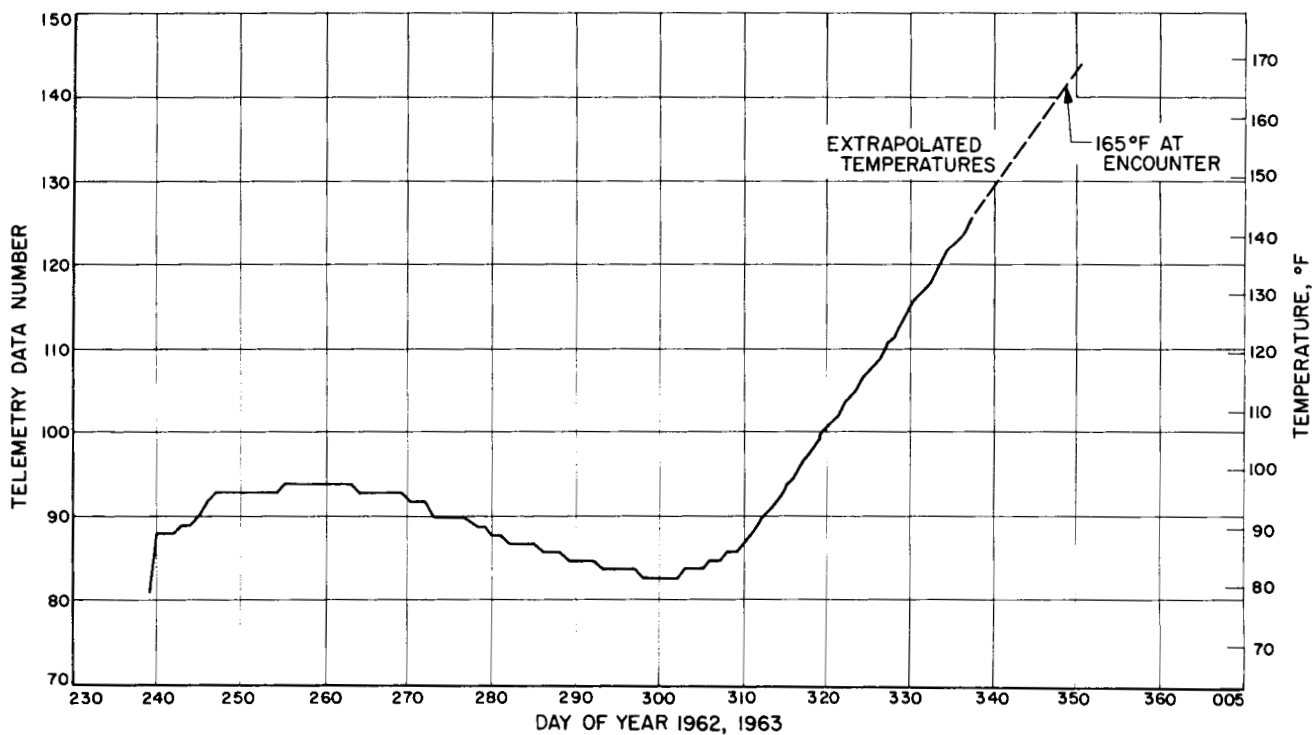


Fig. A-6. *Mariner 2* Earth-sensor temperature

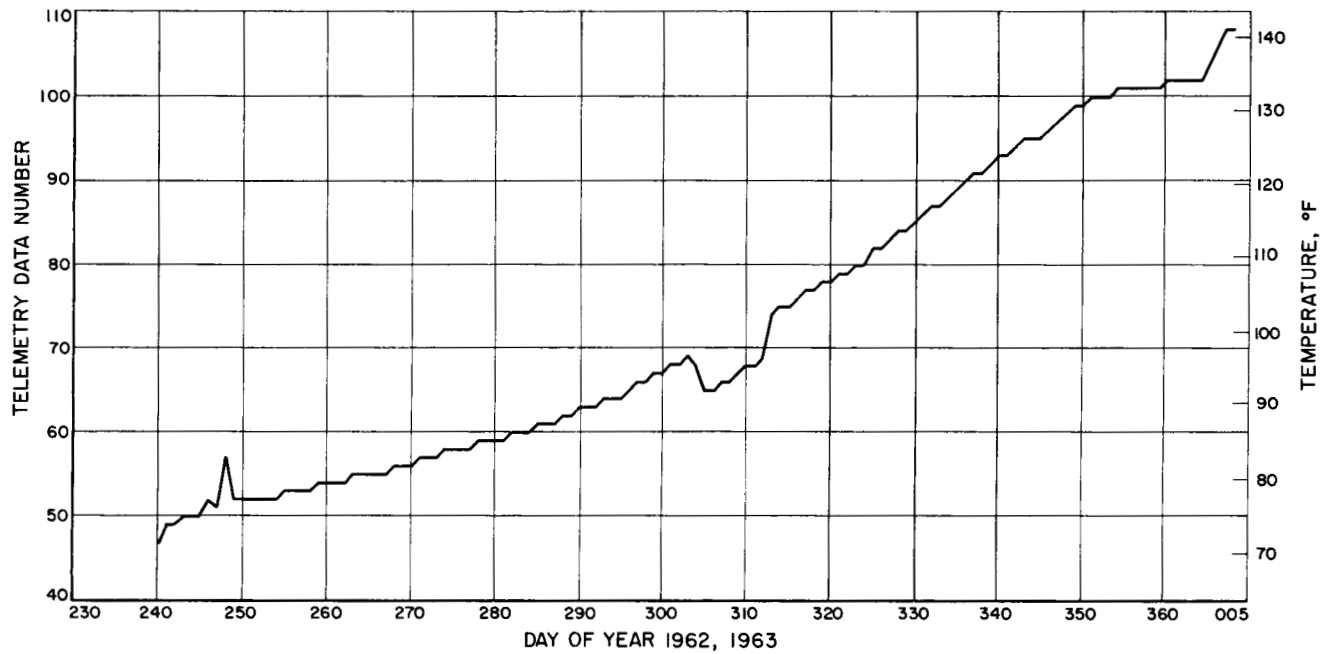


Fig. A-7. *Mariner 2* battery temperature

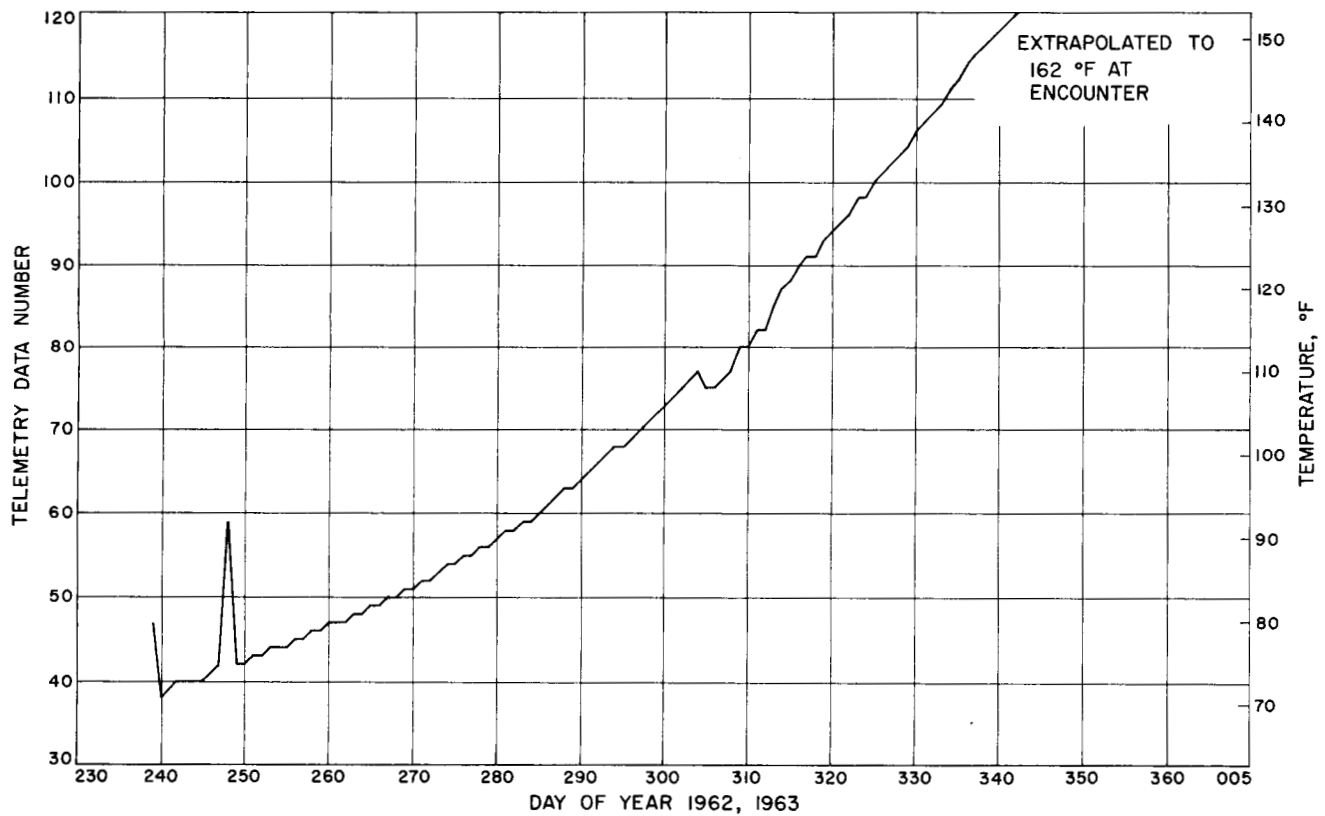


Fig. A-8. *Mariner 2* attitude-control system nitrogen-tank temperature

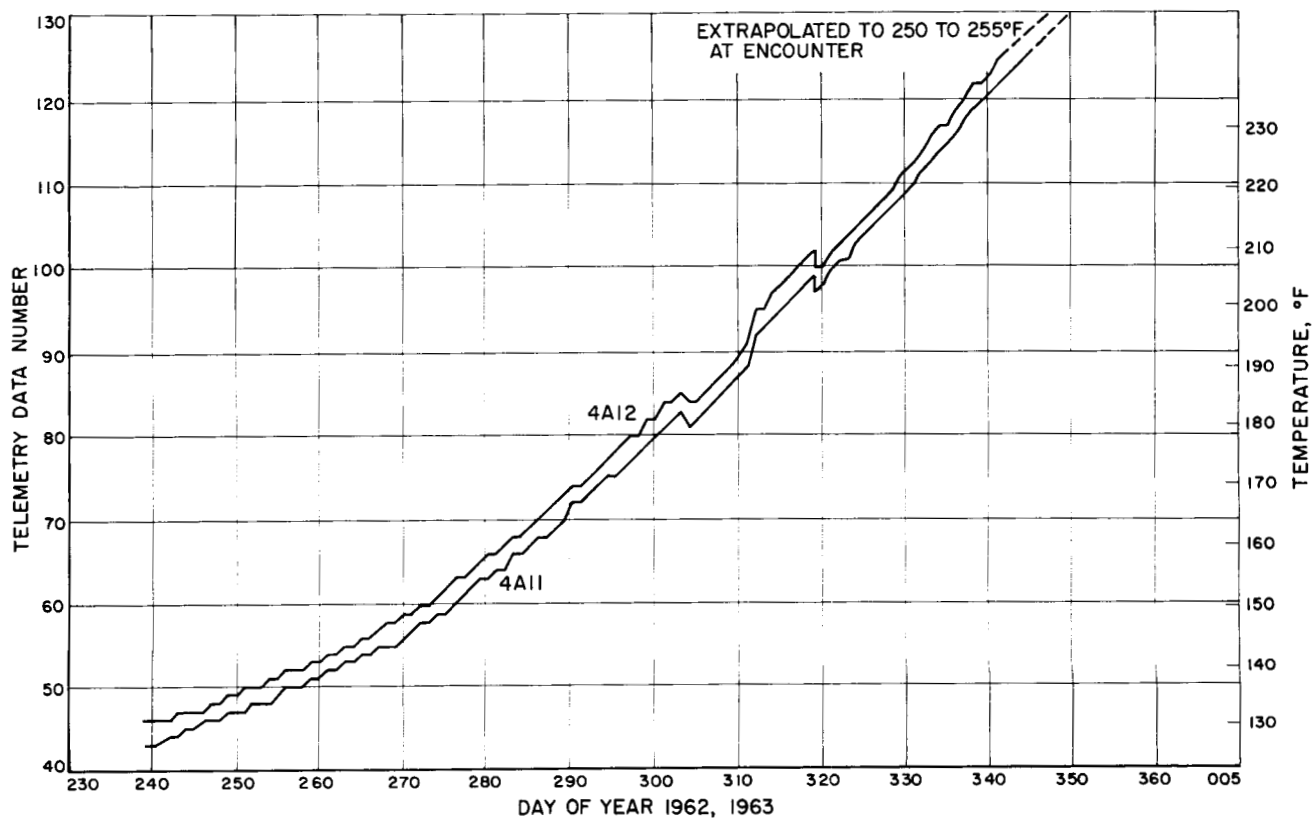


Fig. A-9. Mariner 2 4A11 and 4A12 solar-panel front temperatures

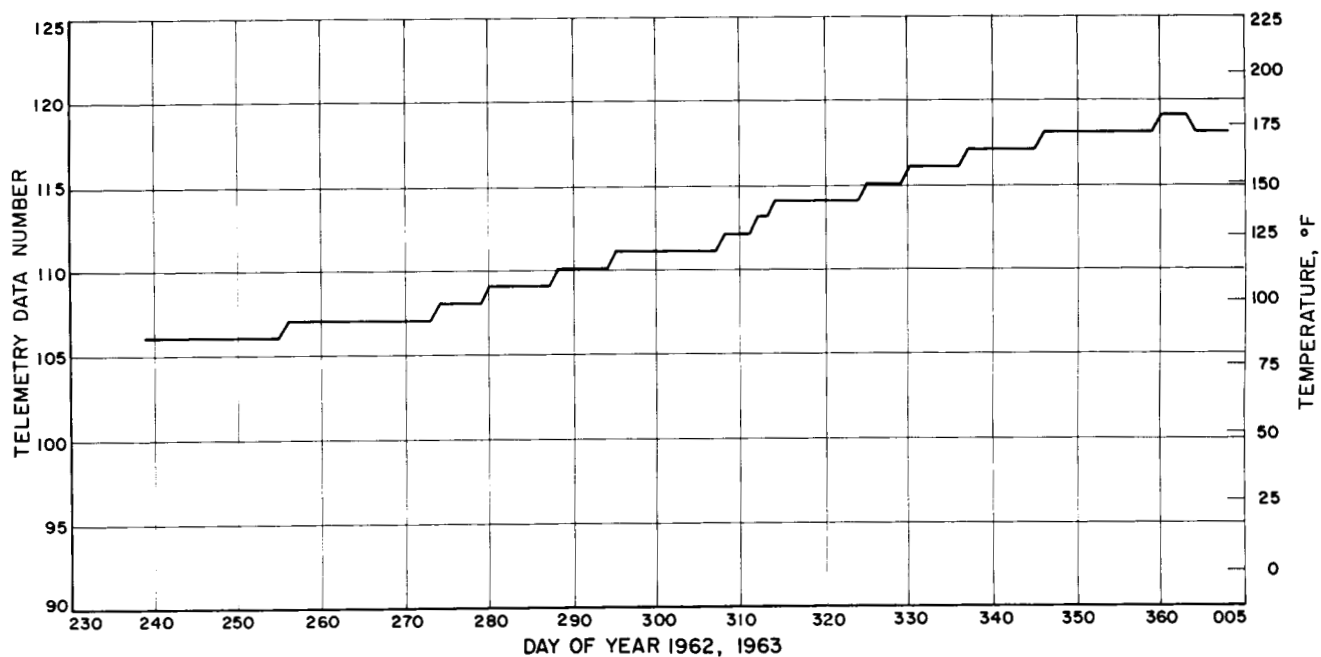


Fig. A-10. Mariner 2 4A11 solar-panel back temperature

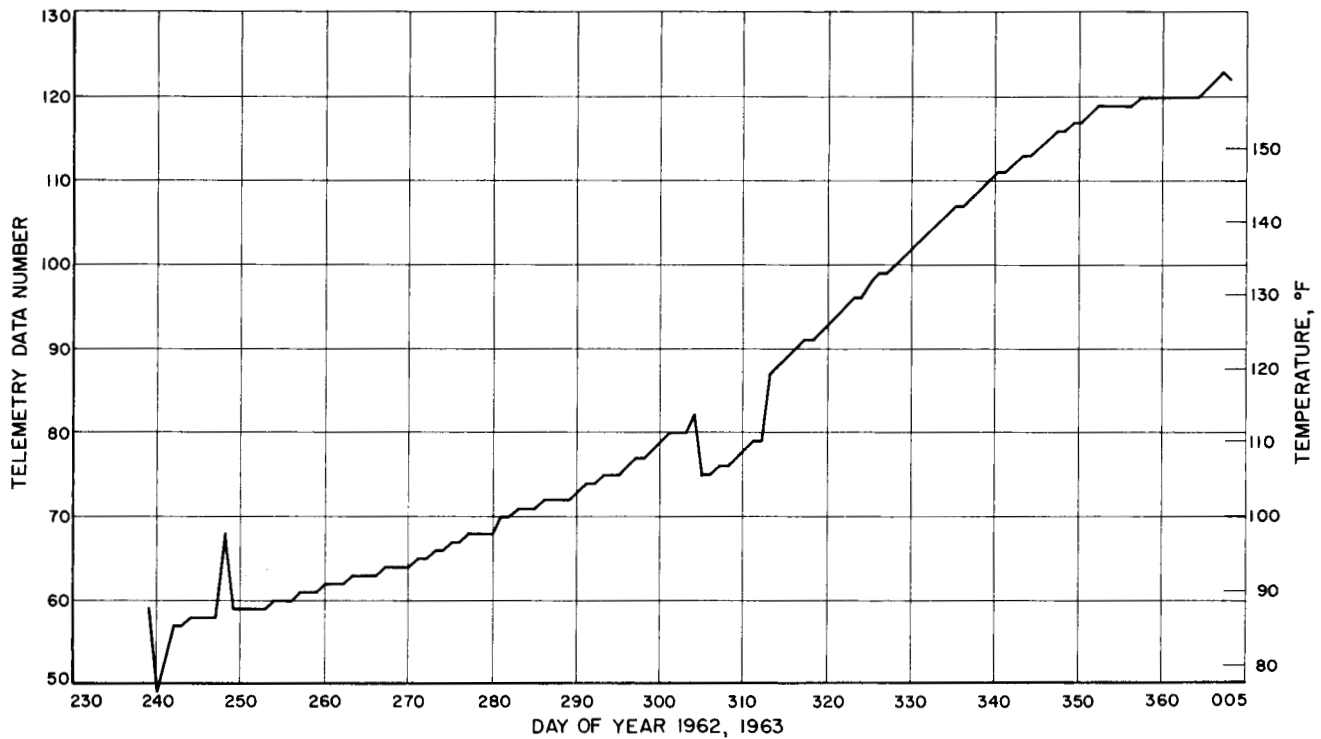


Fig. A-11. *Mariner 2* electronic assembly I temperature (power boost-regulator and science assemblies)

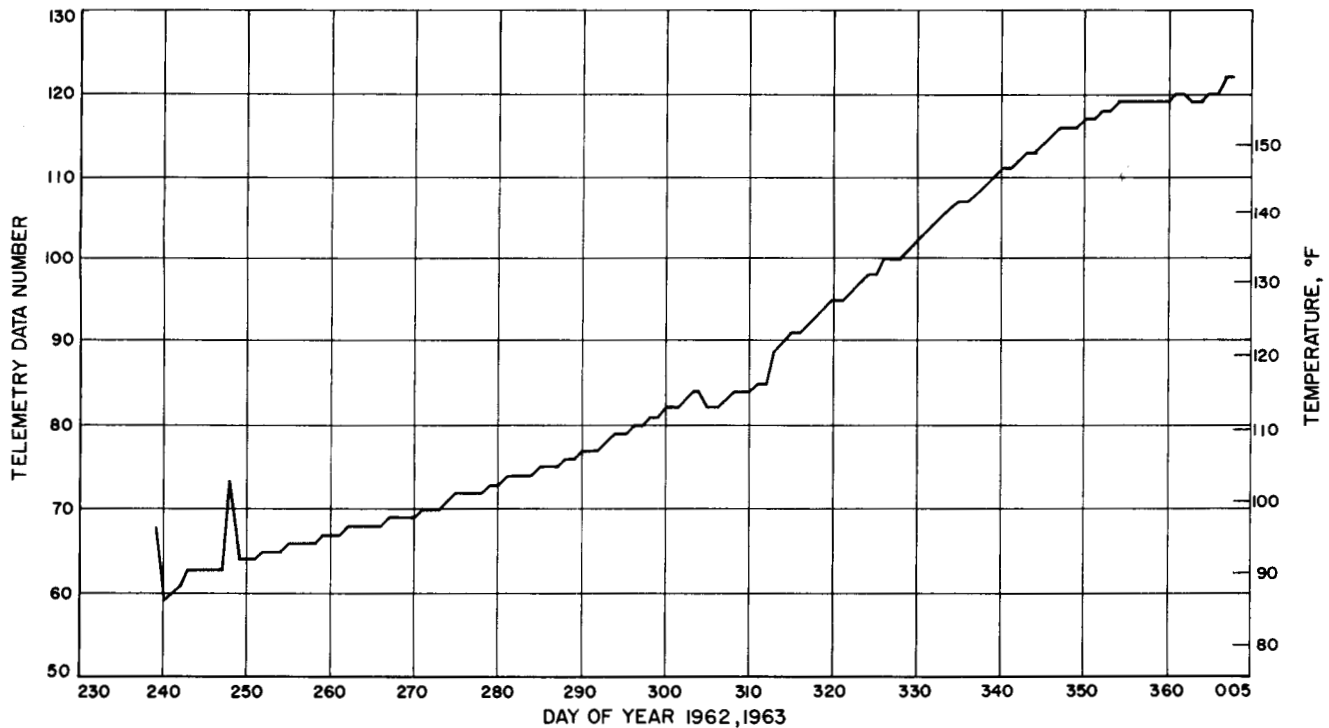


Fig. A-12. *Mariner 2* electronic assembly II temperature (transponder)

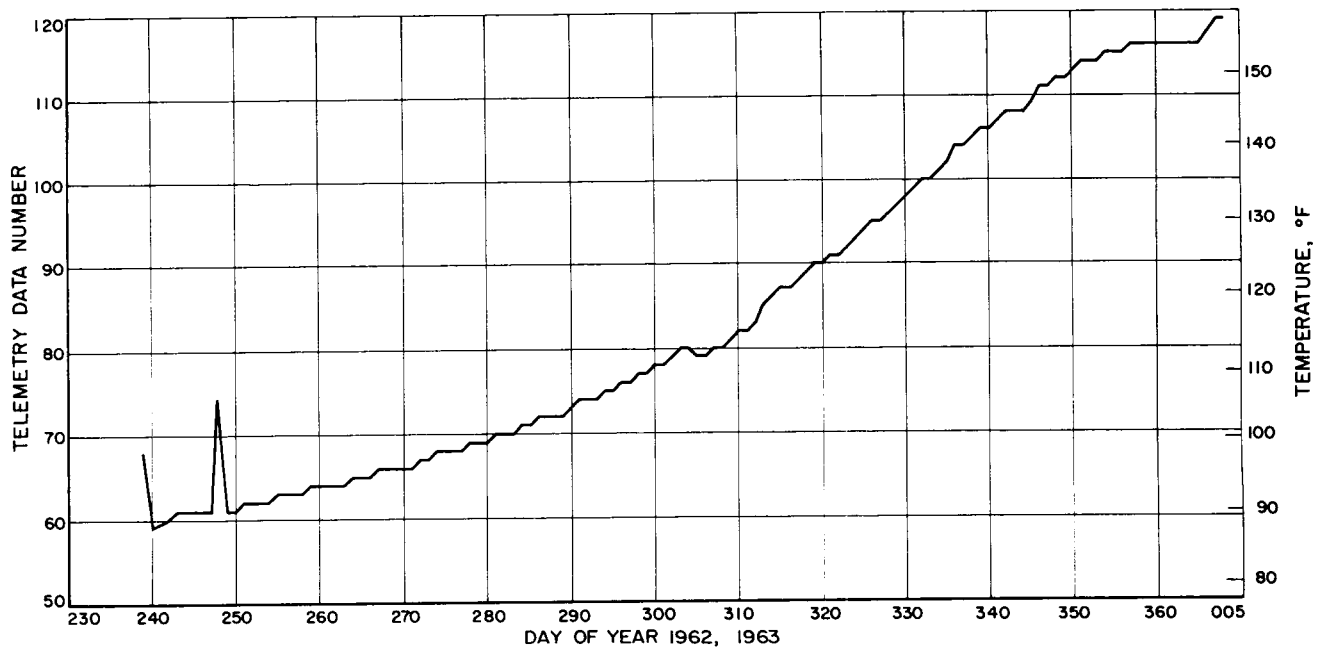


Fig. A-13. *Mariner 2* electronic assembly III temperature (data encoder and command)

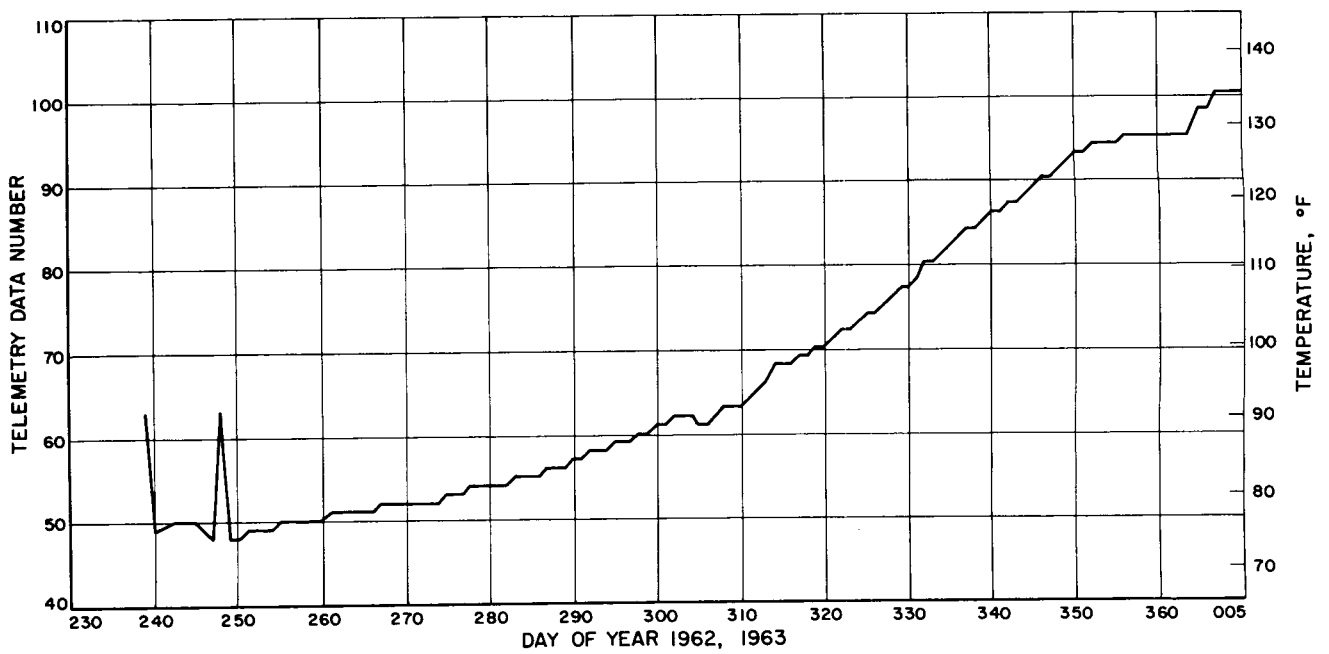


Fig. A-14. *Mariner 2* electronic assembly IV temperature (CC&S and attitude control)

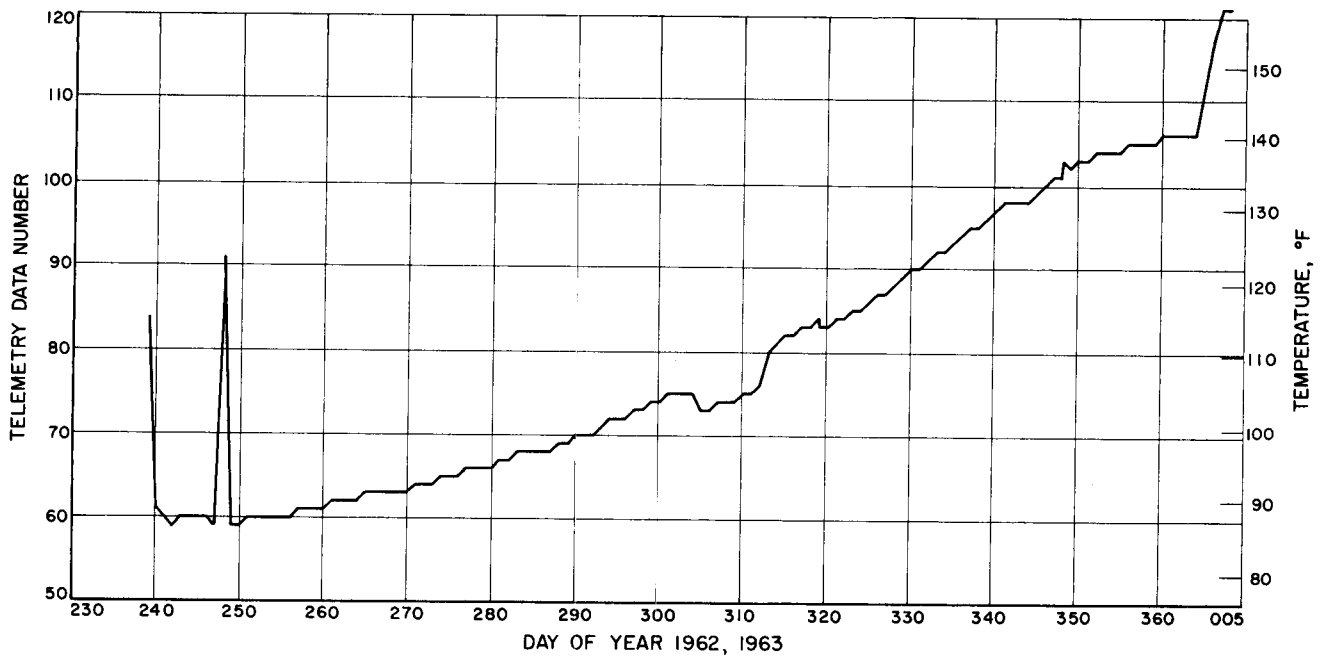


Fig. A-15. *Mariner 2* electronic assembly V temperature (power and pyrotechnics assemblies)

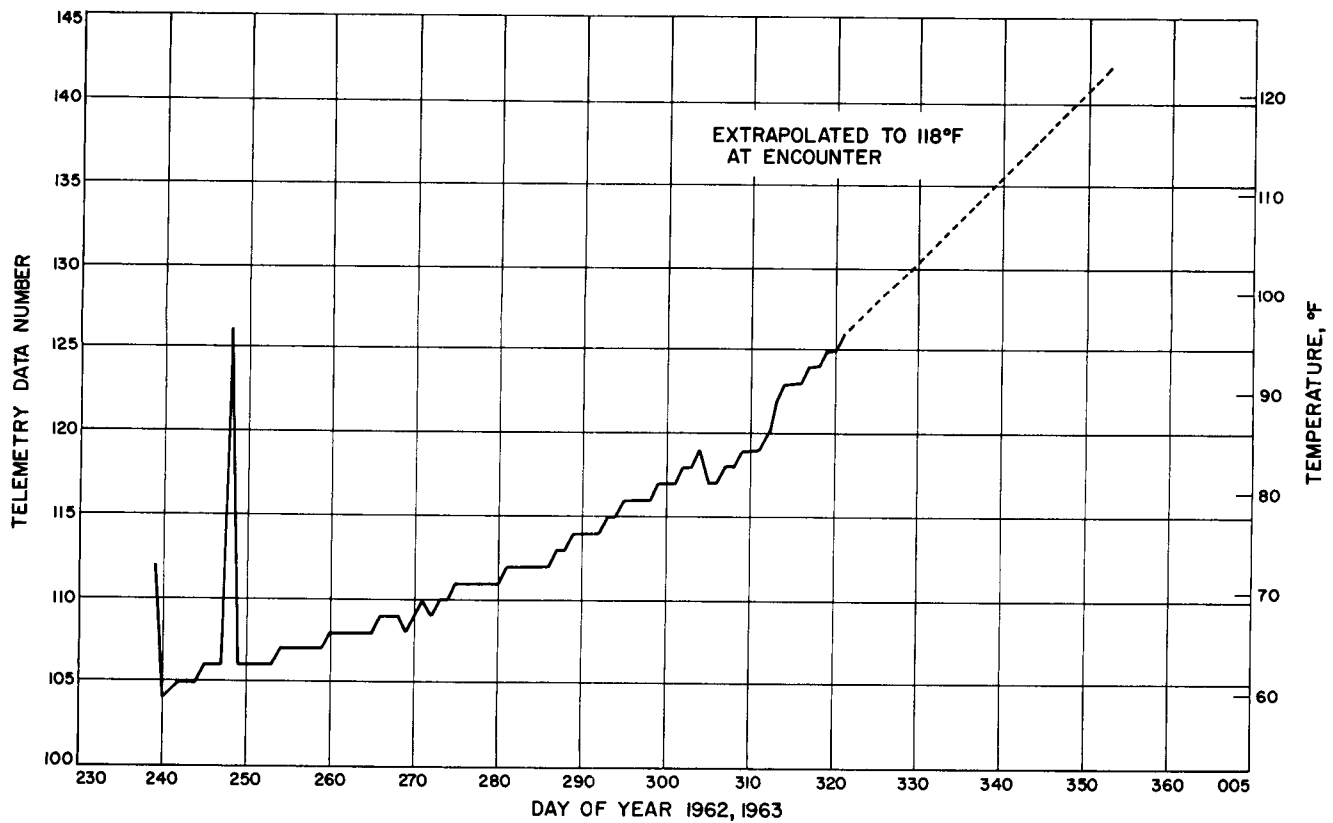


Fig. A-16. *Mariner 2* lower thermal shield temperature

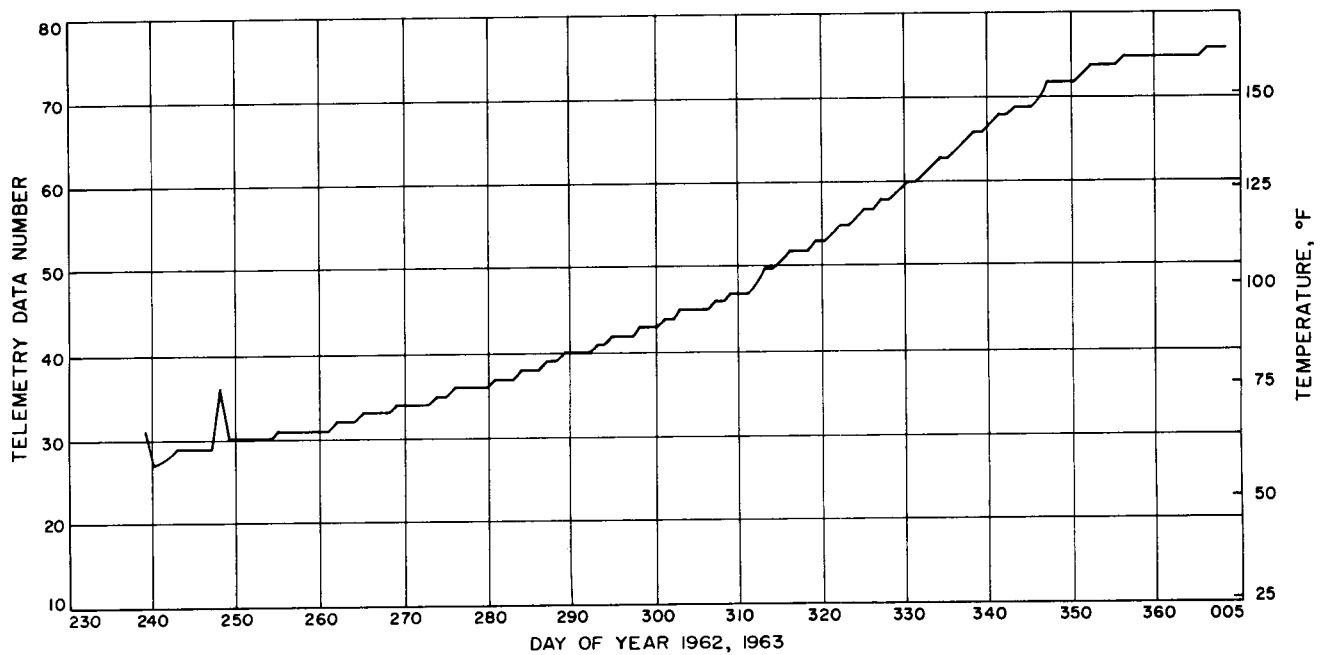


Fig. A-17. Mariner 2 upper thermal shield temperature

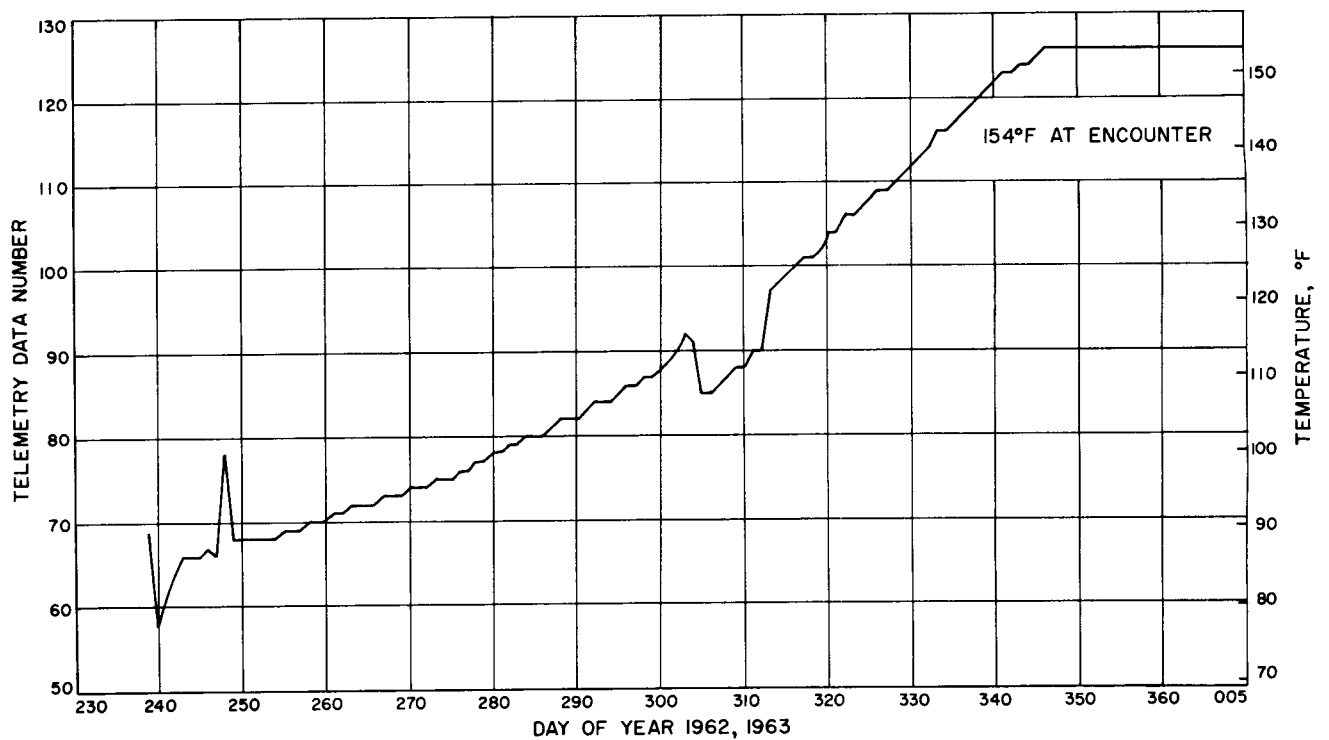


Fig. A-18. Mariner 2 plasma experiment temperature

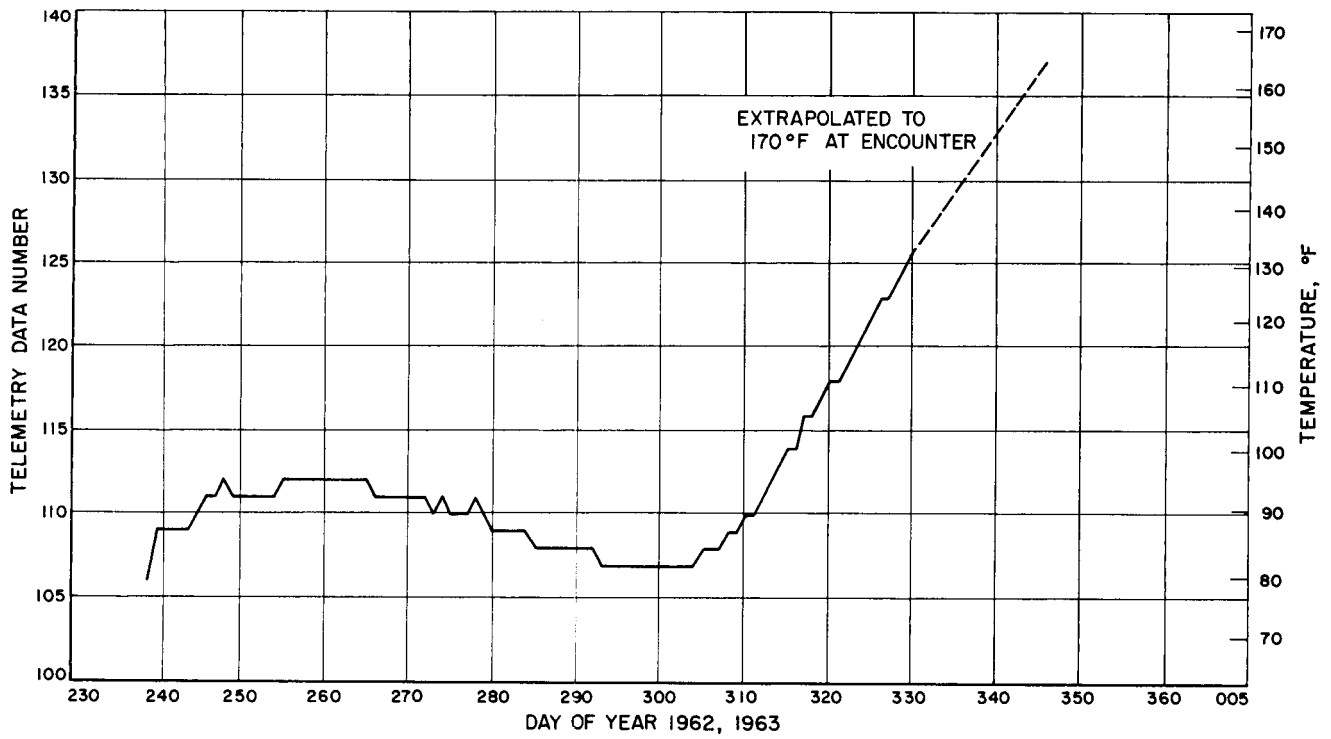


Fig. A-19. *Mariner 2* antenna yoke temperature

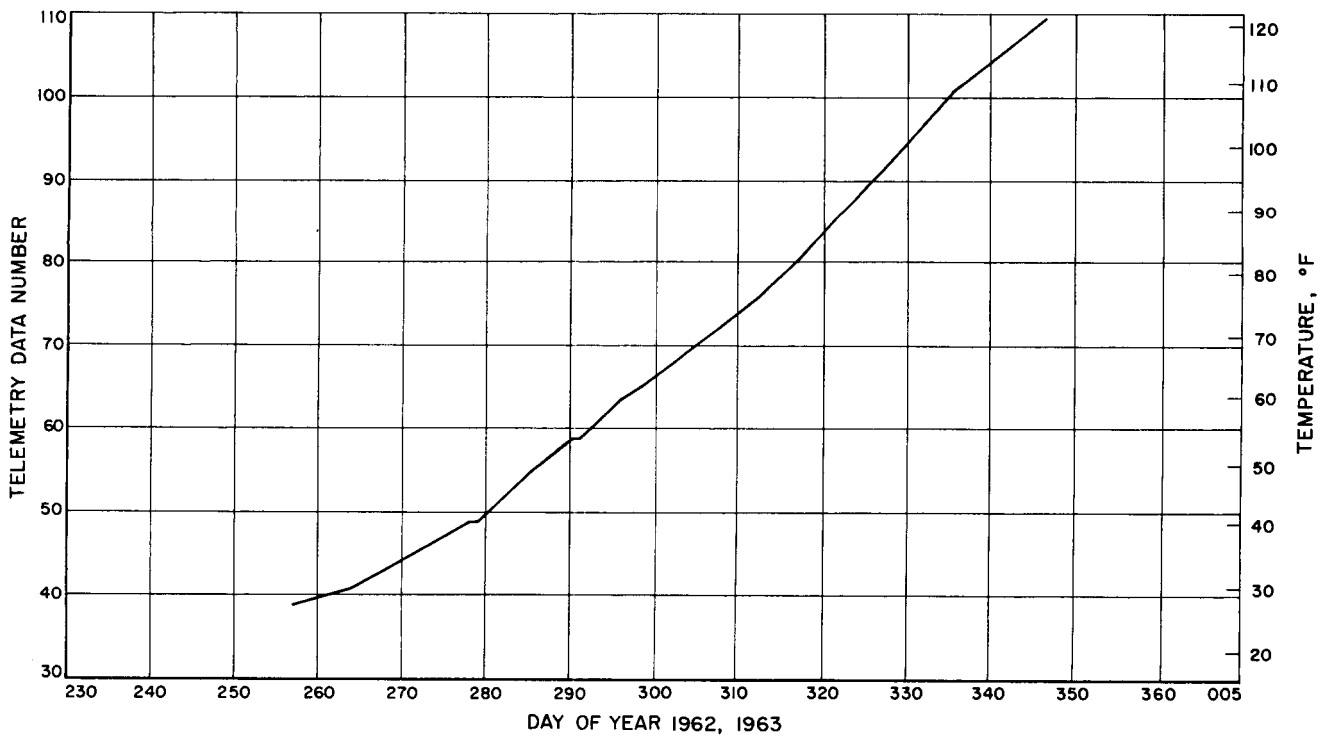


Fig. A-20. *Mariner 2* infrared radiometer housing